Relativistic Outflow of Electron-Positron Pair Plasma from a Wien Equilibrium State

S. Iwamoto and F. Takahara
Department of Earth and Space Science, Graduate School of Science, Osaka University
Machikaneyama 1-1, Toyonaka, Osaka, 560-0043, Japan
iwamoto@vega.ess.sci.osaka-u.ac.jp
takahara@vega.ess.sci.osaka-u.ac.jp

ABSTRACT

We investigate a novel mechanism of bulk acceleration of relativistic outflows of pure electron positron pairs both analytically and numerically. The steady and spherically symmetric flow is assumed to start from a Wien equilibrium state between pure pairs and photons in a compact region which is optically thick to the electron scattering at a relativistic temperature. Inside the photosphere where the optical thickness becomes unity, pairs and photons behave as a single fluid and are thermally accelerated. Outside the photosphere, pairs and photons behave separately and we assume the free streaming approximation for photons, which are emitted from the relativistically moving photosphere. Pairs are shown to be thermally accelerated further even outside the photosphere because the photospheric temperature is at least mildly relativistic. It is to be noted that the mean energy of photons is higher than that of pairs in the comoving frame of pairs and that the Compton interaction leads to additional heating and radiative acceleration of pairs. For a reasonable range of the boundary temperature and optical thickness, the terminal Lorentz factor of pair outflows turns out be more than 10 and the terminal kinetic power accounts for more than 2/3 of the total luminosity. While the total luminosity should be at least larger than the Eddington luminosity, real luminosity can be modest if the outflow is collimated by some unknown mechanisms. This mechanism successfully avoids the difficulties of pair annihilation and radiation drag owing to the pair production by accompanying high energy photons and the strong beaming of radiation field. It is seen that most pairs injected at the boundary survive to infinity. The radiation from the photosphere should be observed as MeV peaked emission at infinity with an order of kinetic power of jets.

Subject headings: electron-positron pairs, hydrodynamics, relativistic plasma, relativistic jets, blazars

1. Introduction

The production and bulk acceleration of relativistic jets in active galactic nuclei is one of the most challenging problems in astrophysics. The basic properties to be explained are the highly relativistic velocity with the bulk Lorentz factor of around 10, the kinetic power almost comparable to the Eddington luminosity, and the collimation into a small opening angle (e.g., Ostrowski et al. 1997; Begelman, Blandford and Rees 1984). Although many ideas have been proposed ranging from magnetic and radiative accelerations to Blandford-Znajek process, each model has its own difficulties and there is no general consensus on how jets are produced and accelerated (e.g., Begelman 1995; Begelman, Blandford and Rees 1984). In this paper, we explore a thermal acceleration mechanism of pure electron-positron plasma in view of the recent observational and theoretical developments.

Several important observational developments have been made in this decade. First of all, EGRET on board the Compton Gamma Ray Ob-

servatory has found that blazars are a strong γ-ray emitter (Mukherjee et al. 1997). The γ-ray emission is interpreted in terms of the inverse Compton scattering off relativistic electrons in the jets the direction of which is so close to the line of sight that the emission from jets is strongly beamed (e.g., Blandford & Königl 1979; Maraschi, Ghisellini and Celotti 1992; Sikora, Begelman and Rees 1994). Combining the synchrotron emission at lower energies, we can estimate the physical states of the emission region in the jets. The results of multi-frequency spectral fitting indicate that the jets are particle dominated rather than magnetic field dominated (Inoue and Takahara 1996; Kino, Takahara and Kusunose 2001). The energy density of relativistic electrons is more than one order of magnitude larger than that of the magnetic field. The size of the emission region is estimated to be $10^{16} \sim 10^{17}$cm from time variabilities and visibility of γ-ray photons. Relativistic beaming factor of around 10 is required to assure the visibility of γ-ray photons. Since the distance of the emission region from the central black hole is reasonably estimated to be 10 times its size, it is around $10^{17} \sim 10^{18}$cm, an order of magnitude shorter than that of superluminal knots observed at radio wavelengths. Thus, the bulk acceleration of jets must occur within such short distances. As for the matter content of jets, electron-positron pair dominance has been proposed based on several independent observations (Wardle et al. 1998; Reynolds et al. 1996; Hirotani et al. 1999, 2001), although the contribution of protons is not completely excluded.

Second important development is the estimation of the kinetic power of extended radio sources. Such studies have shown that large scale kinetic power is well correlated with radiative power and suggest that jets are produced by accretion process rather than they are two unrelated phenomena (Rawlings and Saunders 1991). Related to this, Galactic superluminal sources GRO J1655+40 and GRS 1915+105 with the bulk Lorentz factor of a few were discovered (Hjellming & Rupen 1995; Mirabel & Rodríguez 1994). The jet ejection for these two sources seems to be correlated with X-ray behavior, which suggests that the jets are really produced by accretion (Feroci et al. 1999).

Finally, developments of observations and models of cosmic gamma-ray bursts (GRBs) are quite fascinating. Confirmation of the afterglows of GRBs implies the basic correctness of the fireball model (Piran, Shemi and Narayan 1993; Rees and Mészáros 1992). In this model, GRBs are initiated by the production of a compact high entropy fireball, although no specific mechanism of the production process itself has been widely accepted. The fireball is relativistic thermal plasma, which consists of photons, electron-positron pairs and a small amount of baryons. As the fireball expands, it is thermally accelerated and the temperature drops. When the temperature drops below the electron mass, electron-positron pairs annihilate, but it is still optically thick to the electron scattering because of a small baryon load. Final outcome is that the initial thermal energy is converted to the bulk kinetic energy of baryons attaining the bulk Lorentz factor of $E/M_{\rm b}c^2$, where E and $M_{\rm b}$ are the total energy and baryon mass of the fireball. Inhomogeneities in the fireball are expected to produce internal shocks which are supposed to correspond to GRBs themselves and an impact to ambient matter produces an external shock which corresponds to afterglows. The emission from shocks is ascribed to the particle acceleration by shocks. It is also mentioned that some GRBs are described by jets rather than spherical explosion with respect to the afterglow light curve and energetics.

We believe that the success of the fireball model for GRBs has strong implications for jets in blazars. For blazars, internal shocks correspond to the compact emission regions which are located relatively near the central black hole and external shocks produce large-scale radio sources (Carilli and Barthel 1996; Begelman and Cioffi 1989). But, one strong difference between blazars and GRBs is the size of the fireball. The initial size of GRB fireballs is $10^6 \sim 10^7$ cm and it is in a complete thermal equilibrium for the total energy of $\sim 10^{52}$erg. In contrast, the size of blazar fireballs should be around $3r_{\rm g} \sim 10^{14}$cm with a similar total energy, where $r_{\rm g} \equiv 2GM/c^2$ is the Schwarzshild radius for the black hole mass M; the typical value of M is taken to be $10^8 M_\odot$. If the blazar fireball is in a complete equilibrium, the temperature is an order of 10^5K which is far below the electron mass and no pair production is expected. Basically it describes an optical thick radiation pressure dominated standard accretion

disk and no relativistic expansion is expected.

However, for an optically thin state, electron temperature can be relativistic and copious electron-positron pairs can exist in principle. Even for mildly relativistic temperatures, copious electron-positron pairs exist for a finite optical thickness to scattering (Svensson 1984; Lightman 1982; Kusunose and Takahara 1985). It has been shown that the pair density is limited to a relatively small value in hot accretion disks when the pair production is balanced with pair annihilation (Kusunose and Takahara 1988). However, effect of pair escape can increase the pair density as was exemplified by Yamasaki, Takahara, and Kusunose (1999). They have argued that pair outflow from hot accretion disks may account for major part of the dissipated energy from accretion. In such a state, photons and electron-positron pairs are not in a complete thermal equilibrium but they are coupled by electron scattering and pair production/annihilation process and the photon density is far below that of the equilibrium state for a given temperature. Thus, the escaping pairs just above the disk may act as the fireball to produce relativistic jets. Although the physical state of such escaping pairs has not been fully investigated by now, we believe that this is the most promising way of producing relativistic jets with electron-positron pairs.

In this paper, we consider the bulk acceleration of such fireballs starting from a range of the initial states in the simplest way. We treat steady and spherically symmetric outflows starting from pure electron-positron pairs with photons in a Wien equilibrium for which photon distribution function is given by a Boltzmann distribution with a finite chemical potential. The formulation is similar to that of Grimsrud & Wasserman (1998) (GW98), in which relativistic flows of pure electron-positron pairs starting from a complete thermal equilibrium were analyzed. The dynamics starting from a Wien equilibrium is expected to be similar to that given by GW98 when proper accounts for the difference are taken. This type of flows takes into account of the effects of pair production as well as pair annihilation. Then, we can examine to what extent we can avoid the pair annihilation problem pointed out by some authors arguing against electron-positron pair dominance in relativistic jets (Celotti and Fabian 1993; Blandford and Levinson 1995). If pairs eventually annihilate in the course of expansion, there would remain very little kinetic power. It is very important to quantitatively assess the surviving kinetic power of such a fireball.

In section 2, we give basic formulation, in section 3 we present approximate analytical solutions and in section 4 we present the results of numerical solutions.

2. Formulation

We assume that at the inner boundary the source of pure electron-positron pairs and high energy photons injects a steady outflow of pairs and radiation. The optical thickness of such a region to the electron scattering is large but that to the absorption is smaller than unity. Thus, the physical state of such a regime may be characterized by a Wien equilibrium in the simplest case. When we neglect the dynamical effects, physical state of such a plasma with a finite amount of protons is known to be strongly constrained by thermal balance and pair equilibrium owing to the inefficiency of pair annihilation at relativistic temperatures (Lightman 1982; Svensson 1984; Kusunose and Takahara 1985). However, we should note that the time scale to reach such a steady state is fairly long. If the plasma is first put at a relativistic temperature without pairs, pair production proceeds very quickly and the subsequent photon production and Compton scattering strongly cool the plasma as the pair concentration still increases. Finally, pair annihilation leads to a pair equilibrium state. The time scale to reach the pair equilibrium state is controlled by the photon production and photon escape, the time scales of which are much longer than the dynamical time scale. Thus, the dynamical effects are essential to the behavior of such plasma and most probably lead to the expansion and outflow. The constraints on the electron temperature and optical thickness should be drastically changed from those for static confined plasma. In this paper, for simplicity, we assume that a Wien equilibrium state is already established from the outset and that the temperature and optical thickness can take a wider range than those of static cases. Since the properties of the initial states, where dynamical effects are critically important, are not well known, we here

regard the temperature and optical thickness at the boundary as free parameters.

The flow is optically thick near the boundary and becomes optically thin beyond the photosphere. We treat separately optically thick and thin regimes as GW98. For optically thick regime in which the optical thickness to the electron scattering for radially outgoing photons is larger than unity, we treat as if electron-positron pairs and photons form a single fluid. Although, radiation field may be anisotropic, we simply assume isotropic photon distribution in the comoving frame. Note that as was explicitly shown in GW98, the isotropy of photon field is a surprisingly good assumption in a relativistic expanding flow. Although the assumption of a Wien equilibrium is of course a simplification to treat the dynamical problem in a simple way, we may regard this a reasonable choice for a relativitic expanding flow if the flow start from a Wien equilirium. This is seen in the behavior of the cosmic microwave background radiation in cosmology and the optically thick relativistic wind considered by GW98; the photon distribution remains a Planckian even after the optical thickness becomes much below unity. Anyhow, to obtain more exact photon spectrum, we need to solve the radiative transfer coupled with dynamics, a challenging problem which will be pursued in future. Then, the basic equations are the conservation laws of energy, momentum and numbers. For a steady and spherically symmetric flow, conservation laws of energy and momentum are given by

$$\frac{1}{r^2}\frac{d}{dr}\left[r^2(\rho+P)\Gamma^2\beta\right]=0 \tag{1}$$

and

$$\frac{1}{r^2}\frac{d}{dr}\left[r^2(\rho+P)\Gamma^2\beta^2\right]+\frac{dP}{dr}=0, \tag{2}$$

respectively. Here, ρ and P are the total energy density and pressure of electron-positron pairs and photons. Both components are described by ideal fluids and we use the units of $c=1$. The bulk flow velocity and its Lorentz factor are denoted by β and Γ, respectively. Momentum conservation law is alternatively written by

$$\frac{1}{\Gamma}\frac{d\Gamma}{dr}+\frac{1}{\rho+P}\frac{dP}{dr}=0. \tag{3}$$

The energy density and pressure of electron-positron pairs are given by

$$\rho_{\rm e\pm}=2m_{\rm e}n_{\rm e}\langle\gamma\rangle \tag{4}$$

and

$$P_{\rm e\pm}=2m_{\rm e}n_{\rm e}\theta, \tag{5}$$

respectively. Here, $n_{\rm e}$ is the number density of electrons (=that of positrons) and the total number density of leptons are $2n_{\rm e}$, θ is the temperature normalized by the electron mass $m_{\rm e}$ and $\langle\gamma\rangle=K_3(1/\theta)/K_2(1/\theta)-\theta$ is the average Lorentz factor of electron thermal velocity, where K_i is the i-th order modified Bessel function of the second kind.

As was mentioned above, we assume that pairs and photons are in a Wien equilibrium in the initial state. In a Wien equilibrium, the energy density and pressure of photons are given by

$$\rho_\gamma=3m_{\rm e}n_\gamma\theta \tag{6}$$

and

$$P_\gamma=m_{\rm e}n_\gamma\theta, \tag{7}$$

respectively, where n_γ is the number density of photons. In a Wien equilibrium, $n_{\rm e}$ and n_γ are related by

$$\frac{n_e}{n_\gamma}=\frac{K_2(1/\theta)}{2\theta^2}\equiv f(\theta). \tag{8}$$

In numerical calculations of the flow we do not use eq.(8), but solve the following number conservation equations, assuming that pairs and photons take the same temperature,

$$\frac{1}{r^2}\frac{d}{dr}\left[r^2n_{\rm e}\Gamma\beta\right]=\dot{n}_{\rm e} \tag{9}$$

and

$$\frac{1}{r^2}\frac{d}{dr}\left[r^2n_\gamma\Gamma\beta\right]=\dot{n}_\gamma, \tag{10}$$

where $\dot{n}_{\rm e}$ is the pair creation rate minus annihilation rate. The pair annihilation rate is approximated by

$$\begin{aligned}(\dot{n}_{\rm e})_{\rm ann} &= \langle\sigma_{\rm ann}v\rangle n_{\rm e}^2 \qquad (11)\\ &= \frac{3}{8}\sigma_T{n_{\rm e}}^2\left[1+\frac{2\theta^2}{\ln(1.12\theta+1.3)}\right]^{-1},\end{aligned}$$

where v denotes the thermal velocity of pairs (Svensson 1982). The pair creation rate is given by

$$(\dot{n}_{\rm e})_{\rm cre} = \left(\frac{n_\gamma}{n_{\rm e}}\right)^2 \left[\frac{K_2(1/\theta)}{2\theta^2}\right]^2 (\dot{n}_{\rm e})_{\rm ann}, \quad (12)$$

when the distribution function of photons is a Wien one (Svensson 1984). Since we neglect other photon production processes such as bremsstrahlung, there is a simple relation $2\dot{n}_{\rm e} = -\dot{n}_\gamma$.

Then, we can solve for the bulk velocity, temperature and electron number density from the energy, momentum and number conservation equations given above. As the boundary conditions, we give the bulk velocity, temperature, and electron number density at the inner radius at $r = r_0 = 2r_g$. The optical thick approximation is valid between the inner radius and the photosphere. The radial coordinate of the photosphere $r_{\rm ph}$ is defined by

$$\tau = \int_{r_{\rm ph}}^{\infty} dr\ 2n_e\sigma_T\Gamma(1-\beta) = 1. \quad (13)$$

The optical thickness depends on the direction of the photon and for photons moving oblique to the radial direction the optical thickness is larger than that given above. But within the cone of $1/\Gamma$ around the radial direction the difference is small. Outside the cone, the optical thickness becomes much larger. Since we are treating relativistic outflow, the most relevant is the radial optical thickness.

In the optically thin region we treat pairs and photons separately. For pairs, energy, momentum and number conservation laws are given by

$$\frac{1}{r^2}\frac{d}{dr}\left[r^2(\rho_{\rm e\pm}+P_{\rm e\pm})\Gamma^2\beta\right] = F^0, \quad (14)$$

$$\frac{1}{r^2}\frac{d}{dr}\left[r^2(\rho_{\rm e\pm}+P_{\rm e\pm})\Gamma^2\beta^2\right] + \frac{dP_{\rm e\pm}}{dr} = F^1 \quad (15)$$

and

$$\frac{1}{r^2}\frac{d}{dr}\left[r^2 n_{\rm e}\Gamma\beta\right] = \dot{n}_{\rm e}. \quad (16)$$

The right-hand side of energy and momentum conservation laws denotes the so-called radiative force, which is given through the Lorentz transformation of the radiative force in the fluid frame. The latter for Compton cooling is given by Phinney (1982) and Sikora et al. (1996)

$$(F'^0)_{\rm rad} = -\frac{4}{3}(2n_{\rm e})\sigma_T(\langle\gamma^2-1\rangle - \epsilon_\gamma)T'^{00}_\gamma \quad (17)$$

and

$$(F'^1)_{\rm rad} = (2n_{\rm e})\sigma_T\left\{\frac{1}{3}+\frac{2}{3}\langle\gamma^2\rangle\right\}T'^{01}_\gamma, \quad (18)$$

where ϵ_γ denotes the phenomenological Compton heating term described below and $T^{\mu\nu}_\gamma$ is the energy momentum tensor of radiation field. The prime denotes the quantities in the fluid frame whereas those of the central black hole frame are represented without prime. Lorentz transformation between these frames is described as

$$F^\mu = \Lambda^\mu{}_\nu F'^\nu \text{ and } T^{\mu\nu} = \Lambda^\mu{}_\delta\Lambda^\nu{}_\sigma T'^{\delta\sigma}, \quad (19)$$

where

$$\Lambda^\mu{}_\nu = \begin{pmatrix} \Gamma & \Gamma\beta \\ \Gamma\beta & \Gamma \end{pmatrix}. \quad (20)$$

The Compton heating term is calculated as follows. First, the average energy of photons in the fluid frame ϵ is calculated and the equivalent photon temperature $\theta_\gamma = \epsilon/3$ is defined. Noting that $\langle\gamma^2-1\rangle = 3\theta K_3(1/\theta)/K_2(1/\theta)$, we put

$$\epsilon_\gamma = 3\theta_\gamma\frac{K_3(1/\theta_\gamma)}{K_2(1/\theta_\gamma)}. \quad (21)$$

The radiation field is assumed to be given by the free streaming approximation in the optically thin regime. The photons are emitted from the photosphere and they are relativistically beamed with the Lorentz factor of the photosphere. Although we take account of effects of photons on the dynamics of electrons, we neglect the corresponding change of the photon field for simplicity. The equilibrium Lorentz factor of the radiation field is given by (Sikora et al. 1996)

$$\Gamma_{\rm eq} = \frac{1}{\sqrt{2}}\left(1+\frac{1}{\sqrt{1-\delta^2}}\right)^{1/2}, \quad (22)$$

where

$$\delta = \frac{2T^{01}_\gamma}{T^{00}_\gamma + T^{11}_\gamma}. \quad (23)$$

For F'^0, we also include annihilation cooling term as

$$(F'^0)_{\rm ann} = 2m_{\rm e}\dot{n_e}\langle\gamma\rangle \quad (24)$$

in addition to the Compton cooling and heating term. We neglect other terms such as bremsstrahlung cooling, pair production from the photon field. Thus, our treatment is necessarily simplified to obtain detailed estimate of the final states of the flow, but we believe that the basic features of the flow are not much lost by these simplifications.

3. Analytical solution

In this section we describe analytic approximation, which help to understand the physical situation considered in this paper.

3.1. Dynamics of Wien equilibrium pair plasma

In the optically thick regime, adopting one fluid approximation and assuming that Wien equilibrium (eq.8) is maintained in the flow too, we have two integrals from energy and number conservation laws. The energy conservation is written in the one fluid approximation from eqs. (1),(4),(5),(6),(7)&(8)

$$4\pi r^2 m_{\rm e} n_\gamma \left\{4\theta + 2f(\theta)(\theta + \langle\gamma\rangle)\right\}\Gamma^2\beta = \dot{E}, \tag{25}$$

where $\dot{E}$ is the total luminosity. Since the sum of the number of photons and pairs is assumed to be conserved, we obtain from eqs. (9)&(10)

$$4\pi r^2 n_\gamma \{1 + 2f(\theta)\}\Gamma\beta = \dot{N}, \tag{26}$$

where $\dot{N}$ is the total number flux of photons and leptons.

Dividing eq.(25) by eq.(26), we obtain

$$\Gamma = \frac{\dot{E}}{m_{\rm e}\dot{N}}\frac{1 + 2f(\theta)}{4\theta + 2f(\theta)(\theta + \langle\gamma\rangle)}. \tag{27}$$

In the limit of relativistic temperature, $f(\theta) \to 1$ and $\langle\gamma\rangle \to 3\theta$, then we have

$$\Gamma \to \frac{\dot{E}}{m_{\rm e}\dot{N}}\frac{1}{4\theta}. \tag{28}$$

In the limit of non-relativistic temperature, $f(\theta) \to 0$ and $\langle\gamma\rangle \to 1$, we have the same expression

$$\Gamma \to \frac{\dot{E}}{m_{\rm e}\dot{N}}\frac{1}{4\theta}. \tag{29}$$

It is to be noted that this expression is not an exact one at intermediate temperatures, in contrast to the case of complete thermal equilibrium(GW98). However, we use this as an approximate analytic solution in this section. This relation implies that the bulk Lorentz factor increases as the temperature decreases, i.e., that the plasma is accelerated thermally in compensation of the internal energy. The factor $\dot{E}/m_{\rm e}\dot{N}$ represents the mean energy of particles except for a numerical factor of order unity. Supposing that Γ at the boundary is order of unity, the bulk Lorentz factor attains an order of 10, if the plasma remains optically thick during an order of magnitude drop in the temperature. The temperature at the boundary needs not necessarily be highly relativistic as long as it is high enough to produce pairs. But, it is important to determine the ratio of pairs to photons at various radii. The actual kinetic power of pairs at infinity depends on the amount of surviving pairs too, which is considered in the following subsections.

The photon number density is also represented by the temperature as (for $\Gamma \gg 1$)

$$n_\gamma = \frac{\dot{N}^2}{\dot{E}}\frac{m_{\rm e}}{4\pi r^2}\frac{4\theta + 2f(\theta)(\theta + \langle\gamma\rangle)}{\left\{1 + 2f(\theta)\right\}^2}. \tag{30}$$

At the relativistic temperatures, it becomes

$$n_\gamma = \frac{\dot{N}^2}{\dot{E}}\frac{m_{\rm e}}{4\pi r^2}\frac{4\theta}{3}, \tag{31}$$

while at non-relativistic temperature, it is

$$n_\gamma = \frac{\dot{N}^2}{\dot{E}}\frac{m_{\rm e}}{4\pi r^2}4\theta. \tag{32}$$

The difference of the factor 3 means that at non-relativistic temperatures all the pairs annihilate and are converted to photons. Anyway, the total number flux of photons and electron pairs is conserved and total number density is approximated by

$$n_\gamma + 2n_{\rm e} = \frac{\dot{N}^2}{\dot{E}}\frac{m_{\rm e}}{4\pi r^2}4\theta. \tag{33}$$

Under the approximations of $\Gamma = \dot{E}/4m_{\rm e}\theta\dot{N}$ and the above expression for $n_\gamma + 2n_{\rm e}$, the equation of motion (eq. 3) becomes

$$-\frac{1}{\theta}\frac{d\theta}{dr} + \frac{(1 + 2f(\theta))r^2}{\theta[4\theta + 2f(\theta)(\theta + \langle\gamma\rangle)]}\frac{d}{dr}\left(\frac{\theta^2}{r^2}\right) = 0. \tag{34}$$

Thus, both for relativistic and non-relativistic temperatures, we obtain

$$\theta \propto r^{-1}. \tag{35}$$

Then, we obtain $\Gamma \propto r$ and $n_\gamma + 2n_{\rm e} \propto r^{-3}$. Thus, thermal acceleration works for this Wien equilibrium pair outflows.

In order that optical thick condition is satisfied, the optical thickness at the boundary should be at least larger than unity. We suppose that the boundary temperature θ_0 is at least mildly relativistic and the number densities of photons and electrons are comparable ($f(\theta_0) \simeq 1$). Thus, we have

$$\begin{aligned} n_{\gamma,0} \simeq n_{\rm e,0} &\simeq \frac{1}{3}(n_{\gamma,0} + 2n_{\rm e,0}) \\ &= \frac{1}{3}\frac{m_{\rm e}}{\pi r_0^2}\frac{\dot{N}^2}{\dot{E}}\theta_0 \\ &\sim \frac{1}{48\pi m_{\rm e}}\frac{\dot{E}}{r_0^2\theta_0{\Gamma_0}^2}. \end{aligned} \tag{36}$$

From eq.(13), the optical thickness at the boundary is estimated as

$$\tau_0 \simeq \frac{n_{\rm e,0}\sigma_T r_0}{3\Gamma_0} \simeq \frac{1}{72}\frac{r_g}{r_0}\frac{m_{\rm p}}{m_{\rm e}}\frac{1}{{\Gamma_0}^3\theta_0}\frac{\dot{E}}{L_{\rm Edd}}, \tag{37}$$

where the Eddington luminosity is defined by

$$L_{\rm Edd} \equiv 2\pi\frac{m_{\rm p} r_{\rm g}}{\sigma_T} \tag{38}$$

and $r_{\rm g}$ is the gravitational radius. Thus, in order to realize $\tau_0 \gg 1$, the total luminosity should be at least an order of the Eddington luminosity for reasonable ranges of Γ_0 and θ_0 at the boundary $r_0 = 2r_{\rm g}$.

The optical thick solution obtained in this subsection is summarized as

$$\Gamma = \Gamma_0\frac{r}{r_0}, \tag{39}$$

$$\theta = \theta_0\frac{r_0}{r} \tag{40}$$

and

$$n_\gamma + 2n_{\rm e} = 3n_{\rm e,0}(\frac{r_0}{r})^3. \tag{41}$$

3.2. Photosphere and freeze-out radius

The optical thickness decreases with radius and the flow eventually becomes optically thin. For relativistic temperatures, the optical thickness is given by

$$\tau \simeq \frac{n_{\rm e}\sigma_T r}{3\Gamma} \simeq \frac{n_{\rm e,0}\sigma_T r_0}{3\Gamma_0}\left(\frac{r}{r_0}\right)^{-3} \equiv \tau_0\left(\frac{r}{r_0}\right)^{-3}. \tag{42}$$

Defining the radius of the photosphere $r_{\rm ph}$ as the radius where $\tau = 1$, we obtain

$$r_{\rm ph} \simeq \tau_0^{1/3} r_0. \tag{43}$$

The temperature at the photosphere $\theta_{\rm ph}$ is

$$\theta_{\rm ph} \simeq \theta_0\tau_0^{-1/3}. \tag{44}$$

If $\theta_{\rm ph}$ is smaller than unity, the real photospheric radius is smaller than $r_{\rm ph}$ given above because $n_{\rm e}$ becomes smaller than n_γ.

On the other hand, equating annihilation time scale with dynamical time scale, we obtain the freeze-out radius $r_{\rm fr}$ as

$$\begin{aligned} &\frac{n_{\rm e}}{(\dot{n_{\rm e}})_{\rm ann}} \simeq \frac{r_{\rm fr}}{\Gamma} \\ \Rightarrow \quad & r_{\rm fr} \simeq \left(\frac{9}{8}\tau_0\right)^{1/3} r_0 \simeq \left(\frac{9}{8}\right)^{1/3} r_{\rm ph}. \end{aligned} \tag{45}$$

These two radii are almost the same. Although the above expression for $r_{\rm fr}$ is correct for $\theta_{\rm ph} > 1$, the coincidence of the two radii itself is valid even if $\theta_{\rm ph} < 1$. Thus, copious pairs exist in the optically thick regime because of the photon photon pair production counterbalancing the pair annihilation, unless the temperature becomes too low at $r_{\rm ph}$. In the optically thin regime, a large fraction of pairs can survive because the annihilation time scale becomes longer than the dynamical time scale.

The behavior of the freeze-out depends on the temperature at the photosphere $\theta_{\rm ph}$. For $\theta_{\rm ph} < 1$, the number density of pairs becomes small compared to the photon density but pairs can still carry a significant amount of kinetic power in the rest mass energy. For $\theta_{\rm ph} > 1$, the number density of pairs is comparable to the photon density and the kinetic power of pairs accounts for more than half of the total power. Surviving kinetic power, however, is affected by interactions with radiation

Fig. 1.— Photospheric temperature in the $\dot{E} - \theta_0$ plane. The upper-left region of $\theta_{\rm ph} = 1$ corresponds to the non-relativistic freeze-out with $\theta_{\rm ph} < 1$, while the lower-right region does to the relativistic freeze-out with $\theta_{\rm ph} > 1$. The lines of τ_0 =const. are also depicted.

Fig. 2.— Relation between $\theta_{\rm ann}$ and $\theta_{\rm ph}$. The solution to equation (63) is shown. The dotted line represents $\theta_{\rm ann} = \theta_{\rm ph}$.

and

$$n_{\rm e}^2 - {n_{\rm e,eq}}^2 \approx 2 n_{\rm e,eq} \delta n_{\rm e}. \quad (56)$$

Since the electron number density follows the equation

$$\dot{n}_{\rm e} = -\langle \sigma_{\rm ann} v \rangle \left[{n_{\rm e}}^2 - {n_{\rm e,eq}}^2 \right] = \frac{1}{r^2} \frac{d}{dr} \left[n_{\rm e} r^2 \Gamma \beta \right], \quad (57)$$

we obtain

$$\delta n_{\rm e} \approx -\frac{1}{2 n_{\rm e,eq}} \frac{1}{\langle \sigma_{\rm ann} v \rangle} \frac{1}{r^2} \frac{d}{dr} \left[n_{\rm e,eq} r^2 \Gamma \beta \right]. \quad (58)$$

Since $\Gamma \propto r$ as long as the equilibrium is maintained, we obtain

$$\delta n_{\rm e} \approx -\frac{\Gamma}{2 r \langle \sigma_{\rm ann} v \rangle} \left[3 + \frac{d \ln n_{\rm e,eq}}{d \ln r} \right] \quad (59)$$

to the leading order. From equation (33), equilibrium number density of electrons is estimated as

$$\begin{aligned} n_{\rm e,eq} &= \frac{\theta m_{\rm e} \dot{N}^2}{\pi r^2 \dot{E}} \frac{f(\theta)}{2 f(\theta) + 1} \\ &\sim \frac{m_{\rm e} \dot{N}^2}{\pi r^2 \dot{E}} \sqrt{\frac{\pi g(\theta)}{8\theta}} \exp(-\frac{1}{\theta}). \end{aligned} \quad (60)$$

Then, equation (59) can be approximated as

$$\delta n_{\rm e} \sim -\frac{\Gamma}{2 r \langle \sigma_{\rm ann} v \rangle} \left[\frac{3}{2} - \frac{1}{\theta} \right] \sim \frac{\Gamma}{2 r \langle \sigma_{\rm ann} v \rangle} \frac{1}{\theta} \quad (61)$$

for $\theta \ll 1$.

We regard that the freeze-out occurs when $\delta n_{\rm e} = n_{\rm e,eq}$ is satisfied. We define the annihilation radius $r_{\rm ann}$ as the radius where $\delta n_{\rm e} = n_{\rm e,eq}$ is satisfied to discriminate it from $r_{\rm fr}$ and $r_{\rm ph}$. The temperature at $r_{\rm ann}$ is denoted by $\theta_{\rm ann}$. The equation to determine $r_{\rm ann}$ and $\theta_{\rm ann}$ is given by

$$\frac{m_{\rm e} \dot{N}^2}{\pi r_{\rm ann}^2 \dot{E}} \sqrt{\frac{\pi}{8\theta_{\rm ann}}} \exp(-\frac{1}{\theta_{\rm ann}}) = \frac{\Gamma_{\rm ann}}{2 r_{\rm ann} \langle \sigma_{\rm ann} v \rangle} \frac{1}{\theta_{\rm ann}}. \quad (62)$$

Recalling that $\Gamma_{\rm ann} \simeq \Gamma_0 (r_{\rm ann}/r_0)$ and $r_{\rm ann} = r_0 (\theta_0/\theta_{\rm ann})$ and using equations (36) and (37), we obtain the equation to determine $\theta_{\rm ann}$ as

$$\theta_{\rm ann}^{5/2} \exp(-\frac{1}{\theta_{\rm ann}}) = \frac{16}{27\sqrt{2\pi}} \frac{\theta_0^3}{\tau_0} = \frac{16}{27\sqrt{2\pi}} \theta_{\rm ph}^3. \quad (63)$$

In Figure 2 the relation between $\theta_{\rm ann}$ and $\theta_{\rm ph}$ is shown and we see that the former is slightly higher than the latter for $\theta_{\rm ph} < 0.6$. The kinetic power of pairs estimated at the annihilation radius is given by

$$\dot{E}_{\rm e\pm,ann} \simeq \dot{E} \frac{f(\theta_{\rm ann})}{\theta_{\rm ann}} \sim \frac{4}{27} \dot{E} (\frac{\theta_{\rm ph}}{\theta_{\rm ann}})^3 \frac{1}{\theta_{\rm ann}^2}. \quad (64)$$

This simple estimate gives a somewhat higher value than that by equation (54). Thus, the kinetic power of pairs is shown to be still fairly high and is comparable to the radiative power even for non-relativistic freeze-out. As for the Lorentz factor at the photosphere, we expect that

$$\Gamma_{\rm ph} \sim \frac{\theta_0}{\theta_{\rm ph}}. \quad (65)$$

The terminal Lorentz factor may be higher by a factor of a few owing to the additional thermal and radiative acceleration in the optically thin regime.

4. Numerical Results

In this section, we present the numerical results which are compared with analytic predictions made in the previous section. Numerical calculations are performed for a wide range of values of the total luminosity $\dot{E}$ and the boundary temperature θ_0 at $r = r_0 = 2r_{\rm g}$. We fix $\Gamma_0 = \sqrt{3/2}$; other boundary values τ_0, $n_{\gamma,0}$ and $n_{\rm e,0}$ and the total number flux $\dot{N}$ are easily obtained through several relations described in the previous section. We solve eqs. (1),(3),(9)&(10) for optically thick regime and eqs. (14),(15)&(16) for optically thin regime. The radiation field in the optically thin regime is calculated in the free streaming approximation as was described in section 2. The photospheric radius which marks the boundary between these two regimes is determined iteratively.

As a typical example of non-relativistic freeze-out, we show in Figure 3 the numerical results for $\dot{E}/L_{\rm Edd} = 24.9$ and $\theta_0 = 2$ with $\tau_0 = 82.4$. Figure 3(a) shows the behavior of the bulk velocity $\Gamma\beta$ and temperature θ. It is seen that the photosphere is located at $r_{\rm ph} = 7.45 r_{\rm g}$ and that the temperature decreases rapidly with radius and becomes $\theta_{\rm ph} = 0.41$ at the photosphere. The bulk Lorentz factor at the photosphere turns out to be $\Gamma_{\rm ph}\beta_{\rm ph} = 5.06$. These numerical values reasonably agree with the analytic predictions of $r_{\rm ph} = 8.7 r_g$, $\theta_{\rm ph} = 0.46$ and $\Gamma_{\rm ph} = 5.3$. In particular, it is seen that a factor of 5 decrease in temperature

matches very well a factor of 5 increase of the bulk Lorentz factor, which confirms the basic feature of the thermal acceleration of the pair plasma in the optically thick regime. The differences between analytic and numerical results may be due to some simplifications made in the analytic estimates such as $\Gamma \gg 1$ and pair annihilation process.

It is particularly important that pair outflow is further accelerated outside the photosphere. The numerical result shows that the terminal Lorentz factor attains $\Gamma_\infty = 15.9$, more than three times that at the photosphere. Most of this factor is accounted for by the internal energy of pairs at the photosphere with an additional effect of radiative acceleration. It should be noted that since even at $\theta_{\rm ph} = 0.41$, $\theta + \langle\gamma\rangle = 2.3$, pure thermal acceleration can attain $\Gamma_\infty \sim 12$. Moreover, beamed photons from the photosphere heat the pairs by Compton interaction since the effective temperature of photons is larger than electron temperature outside the photosphere as is seen in this figure. So the thermal acceleration works efficiently while radiative acceleration also makes a small contribution to bulk acceleration at larger distances. This additional bulk acceleration by a factor of 3 is an important element in comparison with observations.

Figure 3(b) shows the relative number fraction of pairs and photons as a function of the radial coordinate. As is seen, the pair fraction decreases steadily according to the decrease of temperature and annihilation continues to $2r_{\rm ph}$. Thus, the analytic estimate of $r_{\rm fr}$ and $r_{\rm ann}$ may be uncertain within a factor of 2. But, the degree of the decrease is modest and about 20% of pairs annihilate outside the photosphere. To sum up, about 60% of the initial pairs survive in this case. This confirms our prediction that the pair annihilation problem can be avoided when we consider an initial Wien equilibrium state.

Figure 3(c) shows the luminosity of pairs and radiation as a function of the radial coordinate. The total luminosity turns out to remain constant as a function of radius as it should be. Inside the photosphere, the kinetic power of pairs slightly decreases with radius, which is because pairs are converted to photons as the temperature decreases keeping a Wien equilibrium. The kinetic power of pairs is kept almost constant outside the photosphere as it should be for bulk acceleration by their

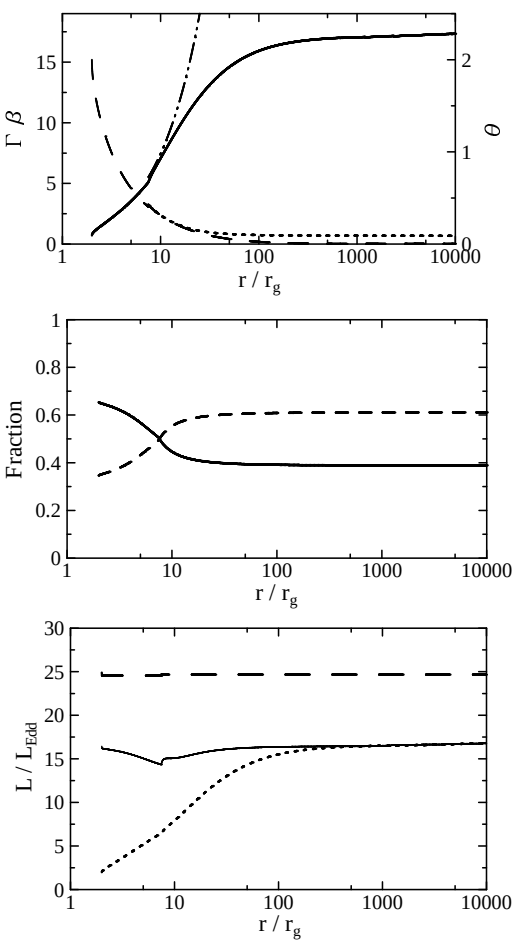

Fig. 3.— (a) Behavior of velocity and temperature for $\dot{E}/L_{\rm Edd} = 24.9$, $\theta_0 = 2$ with $\tau_0 = 82.4$. The solid line denotes the bulk Lorentz factor of the pairs $\Gamma\beta$, and the dash-dotted line denotes the equilibrium Lorentz factor of radiation field $\Gamma_{\rm eq}\beta_{\rm eq}$. The dashed line denotes the temperature of pairs, and dotted line denotes the equivalent temperature of radiation outside the photosphere. (b) Fraction of particle and photon numbers for $\dot{E}/L_{\rm Edd} = 24.9$, $\theta_0 = 2$ with $\tau_0 = 82.4$. The solid and dashed lines denote the number fractions of pairs and photons, respectively. (c) Luminosities of various components for $\dot{E}/L_{\rm Edd} = 24.9$, $\theta_0 = 2$ with $\tau_0 = 82.4$. The dashed line denotes the total luminosity of pairs and radiation. The solid line denotes the kinetic power of pairs while the dotted line denotes the power carried in a form of the rest mass of pairs. Thus, the interval between the dashed and solid lines denotes the luminosity of radiation and that between the solid and dotted lines denotes the power carried in a form of the thermal energy of pairs.

own thermal energy. A small change is due to the interaction with photons. But, it is seen that the energy gained from Compton interaction almost cancels out with a small but finite amount of annihilation cooling. The terminal kinetic power of pairs turns out to be 61% of the total luminosity, while remaining 39% is carried away by photons emitted from the photosphere. Since the matter at the photosphere is moving at $\Gamma = 5$, distant observers see the radiation peaked at an energy of $\Gamma\theta_{\rm ph} \sim 2$, i.e., around 1MeV. Thus, this model predicts that strong MeV emission should accompany the relativistic jet formation.

We have also calculated for various boundary values and the results are tabulated in Table 1. As is seen, the terminal Lorentz factor proves to be $8 \sim 60$ and the terminal kinetic power of pairs accounts for $50 \sim 80\%$ of the total luminosity for $1 < \theta_0 < 5$ and $0.8 < \dot{E}/L_{\rm Edd} < 80$. Thus, the Wien fireball turns out to be quite an efficient mechanism for the production and bulk acceleration of relativistic jets. As for the dependence of the physical quantities at the photosphere, they reasonably agree with the analytic predictions of $r_{\rm ph} \propto \tau_0^{1/3} \propto \dot{E}^{1/3}\theta_0^{-1/3}$, $\theta_{\rm ph} \propto \dot{E}^{-1/3}\theta_0^{4/3}$ and $\Gamma_{\rm ph} \propto \dot{E}^{1/3}\theta_0^{-1/3}$. Figure 4 shows $r_{\rm ph}$ as a function of τ_0 and figure 5 does $\theta_{\rm ph}$ as a function of τ_0 and then, we see that the analytic prediction agrees with numerical results, although the analytic prediction is slightly larger than the numerical result.

Since the enthalpy of pairs at the photosphere is large, pairs are thermally accelerated outside the photosphere. The terminal Lorentz factor is thus basically determined by the boundary temperature for relativistic freeze-out. For non-relativistic freeze-out, additional effect by radiation works to further increase the terminal Lorentz factor. This behavior is clearly seen in Figure 6. The terminal Lorentz factor is above the naive estimate 4θ to a varying degree according to a varying degree of importance of additional thermal and radiative acceleration. It is to be noted that fairly large Lorentz factor can be obtained even for the initial temperature as low as 0.5.

Finally, in Figure 7 is shown the efficiency of the outflow production, i.e., the ratio of the terminal kinetic power of pairs to the total luminosity. It is basically determined by the photospheric temper-

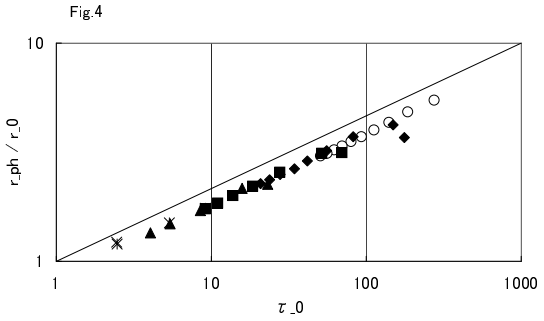

Fig. 4.— Relation between photospheric radius $r_{\rm ph}$ and the initial optical thickness τ_0. The solid line represents the analytic estimate $r_{\rm ph}/r_0 = {\tau_0}^{1/3}$. Open circles, solid diamonds, rectangles, triangles, crosses and stars refer to $\dot{E}/L_{\rm Edd} = 83.1, 24.9, 8.31, 2.49, 0.831$ and 0.249, respectively.

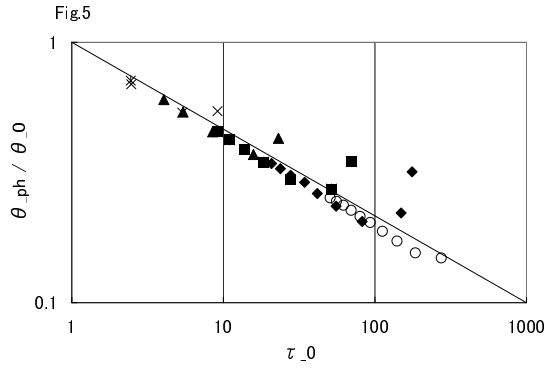

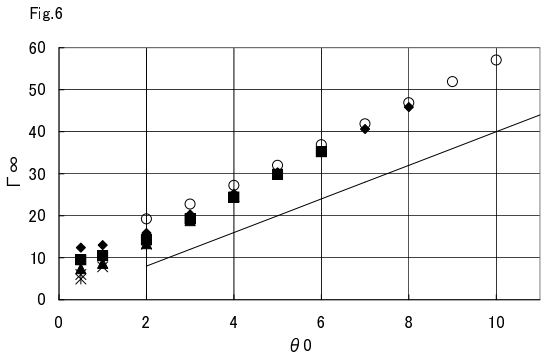

Fig. 5.— Relation between photospheric temperature $\theta_{\rm ph}$ and the initial optical thickness τ_0. The solid line represents the analytic estimate $\theta_{\rm ph}/\theta_0 = {\tau_0}^{-1/3}$. Open circles, solid diamonds, rectangles, triangles, crosses and stars refer to $\dot{E}/L_{\rm Edd} = 83.1, 24.9, 8.31, 2.49, 0.831$ and 0.249, respectively.

Fig. 6.— Terminal Lorentz factor Γ_∞ for various boundary values. The abscissa is the temperature at the boundary θ_0. The symbols are the same as Fig. 4. The solid line represents a naive expectation of $\Gamma_\infty = 4\theta_0$.

ature. For relativistic freeze-out, the efficiency is about 10% larger than the canonical value of 2/3. This excess is due to additional radiative acceleration. For non-relativistic freeze-out, the efficiency becomes small because pair density decreases owing to pair annihilation. At $\theta_{\rm ph} = 0.2$ the efficiency is about 30% and it will be very small for lower $\theta_{\rm ph}$.

Summarizing these results, we have found that electron-positron pairs can be thermally accelerated up to the bulk Lorentz factor of more than 10 and that their kinetic power becomes comparable to the total power, provided that Wien equilibrium states of pure electron-positron pairs are prepared at the inner boundary with a temperature of a few times electron mass and the optical thickness to the scattering of more than around 5. The corresponding total luminosity exceeds the Eddington luminosity by a factor of more than unity in the spherical symmetry. If we assume that the outflow is conical and that the opening angle of the outflow covers Ω steradian, the total power is smaller by a factor of $4\pi/\Omega$. Since Ω is typically as small as 10^{-2}, the required total luminosity can be as small as 1% of the Eddington luminosity. The mechanisms of the realization of pure electron-positron pairs and initial collimation of the outflow remain to be a theoretical challenge. However, we believe that this is the most successful specific mechanism of the bulk acceleration of relativistic outflow up to the Lorentz factor of 10 with high efficiency. This Wien fireball model predicts that radiation from the photosphere should appear as a strong emission around a few MeV with a comparable luminosity to the jet kinetic power.

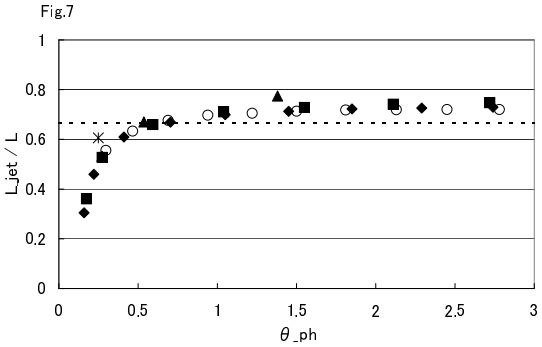

Fig. 7.— Efficiency of the outflow production; i.e., the ratio of the terminal kinetic power of pairs to the total luminosity. The abscissa is the photospheric temperature. The symbols are the same as in Fig. 5. The dotted line refers to the efficiency of 2/3.

5. Discussion

Finally, we discuss several issues related to the Wien fireball model. The first problem is the realization of the initial state. Most probably such a state is prepared in relation to the hot accretion disks or hot accretion disk corona. Previous studies on pair concentration in accretion disks have shown that the pair concentration in the disk is not so large under the steady state condition and that the steady state solution does not exist when the luminosity is higher than about a few percent of the Eddington luminosity (Kusunose and Takahara 1988). This is due to the ineffi-

ciency of the pair annihilation and suggests that pair runaway occurs for such high luminosity. Instead of the pair equilibrium condition, if we allow free escape of pairs from the disk, Yamasaki, Takahara, and Kusunose (1999) have shown that much higher pair concentration is obtained and that outflow luminosity of pairs can be very large based on a simple analysis. This seems to be a promising way to produce the initial state of the present outflow model, since Yamasaki, Takahara, and Kusunose (1999) predicts the optical thickness of pairs is around a few and the temperature of a few. Although pure pair escape was assumed in Yamasaki, Takahara, and Kusunose (1999), in reality baryon load should be carefully examined. If the baryon density is more than 1% of the pair density, the terminal Lorentz factor will be significantly decreased. This is a common problem with the thermal fireball for GRBs.

As for the photon field, we assumed that Wien equilibrium photons are prepared at the boundary and subsequent photon production process is neglected except for pair annihilation. If the initial optical thickness is so large, this seems to be a fair assumption but for optically thickness of a few to 10, this is not true and photon spectrum will not be a Wien one but near the Comptonized bremsstrahlung. Moreover, in order to have a large pair concentration, the amount of soft photons must be small because they will decrease the electron temperature and pair production. In any case, radiative transfer including such as bremsstrahlung and Compton scattering should be examined in a future work. This is also important to predict the accompanying photon spectrum with jet production. It is to be noted that whole process should be treated dynamically, since the pair escape is the most critical assumption for this mechanism.

Our calculation indicates that super Eddington luminosity is needed for an relativistic jet production provided that the flow is spherically symmetric. As was mentioned in the previous section, if some collimation mechanisms exist near the boundary, the required luminosity will be smaller and the real luminosity can be sub-Eddington.

For many years, radiative bulk acceleration mechanism has been regarded ineffective in producing relativistic jets. But most of them treat optically thin case (Phinney 1982; Inoue and Takahara 1996). Since the equilibrium Lorentz factor of photons emitted from typical accretion disks is not large enough near the accretion disk, radiative force acts as radiation drag rather than as acceleration. So the attainable Lorentz factor of bulk flow is at most about 3. This is because radiation field is not collimated enough to the jet direction. Further, for optically thin plasma, only a small fraction of the radiation power is converted to plasma kinetic power. Thus, the optically thin radiative acceleration is ineffective in general. In contrast, our present model assumes that the pair plasma starts to flow out with optically thick condition. This means that photons move at the same speed with pairs since they are strongly coupled and that they can be thermally accelerated. Although the pair outflow becomes optically thin outside the photosphere, radiative acceleration acts effectively because radiation has been collimated at the photosphere and the equilibrium Lorentz factor becomes large enough. Of course, the radiation drag from ambient photons will somewhat decrease the bulk velocity of the jets, but the effect will be small since the beamed radiation field dominates over ambient photons for typical cases.

Another argument against pair jets has been the annihilation problem (Celotti and Fabian 1993; Blandford and Levinson 1995). When a large amount of cold pairs exist in a compact region, they will inevitably annihilate before they escape. Since in our model pairs are hot and accompanied with high energy photons, pair production works as well. Inside the photosphere, pair annihilation is balanced with pair production and outside the photosphere annihilation time scale becomes longer than the dynamical time scale. Thus, the most pairs can survive to infinity and can avoid the annihilation problem with pair jets.

This work is supported in part by the Grant-in-Aid for Scientific Research of the Ministry of Education and Science No.11640236 and by Research Fellowships of the Japan Society for the Promotion of Science.

REFERENCES

Begelman, M. C., Blandford, R. D. and Rees, M. J. 1984, Rev.Mod.Phys. , 56, 255

Begelman, M. C. 1995, Proc.Natl.Acad.Sci.USA,

92, 11442

Begelman, M. C. and Cioffi, D. F. 1989, ApJ, 345, L21

Blandford, R. D. and Königl, A. 1979, ApJ, 232, 34

Blandford, R. D. and Levinson, A. 1995, ApJ, 441, 79

Carilli, C. L. and Barthel, P. D. 1996, A&ARev. , 7, 1

Celotti, A. and Fabian, A. C. 1993, MNRAS, 264, 228

Feroci, M.,Matt, G., Pooley, G., Costa, E., Tavani, M. and Belloni, T. 1999, A&A, 351, 985

Grimsrud, O. M., and Wasserman, I. 1998, MNRAS, 300, 1158 (GW98)

Hirotani, K., Iguchi, S., Kimura, M. and Wajima, K. 1999, PASJ, 51, 263

Hirotani, K., Iguchi, S., Kimura, M. and Wajima, K. 2001, ApJ, 545, 100

Hjellming, R. M. and Rupen, M. P., 1995, Nature, 375, 464

Inoue, S. and Takahara, F. 1996, ApJ, 463, 555

Kino, M., Takahara, F. and Kusunose, M. 2001, ApJ, submitted

Kusunose, M. and Takahara, F. 1985, *Prog.Theor.Phys.*, 73, 41

Kusunose, M. and Takahara, F. 1988, PASJ, 40, 435

Lightman, A. P. 1982, ApJ, 253, 842

Maraschi, L., Ghisellini, G. and Celotti, A. 1992, ApJ, 397, L5

Mirabel, I. F. and Rodríguez, L. F. 1994, Nature, 371, 46

Mukherjee, R. et al. 1997, ApJ, 490, 116

Ostrowski, M., Sikora, M., Madejski, G. and Begelman, M. 1997 Relativistic Jets in AGNs (Jagelonian Observatory, Cracow)

Phinney, E. S. 1982, MNRAS, 198, 1109

Piran, T., Shemi, A. and Narayan, R. 1993, MNRAS, 263, 861

Rees, M. J. and Mészáros, P. 1992, MNRAS, 258, 41p

Reynolds, C.S., Fabian, A.C., Celotti, A., and Rees, M.J. 1996, MNRAS, 283, 873

Rawlings, S. and Saunders, R. 1991, Nature, 349, 138

Sikora, M., Begelman, M. C. and Rees, M. J. 1994, ApJ, 421, 153

Sikora, M., Sol, H., Begelman, M. C. and Madejski, M. G. 1996, MNRAS, 280, 781

Svensson, R. 1982, ApJ, 258, 335 (1982)

Svensson, R. 1984, MNRAS, 209, 175

Wardle, J. F. C., Homan, D. C., Ojha, R. and Roberts, D. H. 1998, Nature, 395, 457

Yamasaki, T., Takahara, F., and Kusunose, M. 1999, ApJ, 523, L21

Table 1

$\dot{E}/L_{\rm Edd}$	θ_0	τ_0	$r_{\rm ph}$	$\Gamma_{\rm ph}\beta_{\rm ph}$	$\theta_{\rm ph}$	$\Gamma_\infty\beta_\infty$	$L_{\rm jet}$	$L_{\rm jet}/\dot{E}$
0.249	0.5	2.45	2.45	1.30	0.356	4.95	0.151	0.606
0.831	0.5	9.15	3.50	1.94	0.272	6.00	0.442	0.532
0.831	1	5.36	3.00	1.87	0.537	7.84	0.557	0.670
0.831	2	2.47	2.40	2.30	1.38	13.2	0.643	0.774
2.49	0.5	23.1	4.51	2.52	0.214	7.40	1.10	0.443
2.49	1	15.8	4.32	2.73	0.371	8.67	1.49	0.600
2.49	2	8.50	3.42	2.38	0.906	13.4	1.78	0.716
2.49	3	5.42	2.97	2.01	1.62	18.9	1.88	0.756
2.49	4	4.05	2.70	1.78	2.41	24.5	1.96	0.786
8.31	0.5	69.7	6.30	3.42	0.174	9.51	3.00	0.361
8.31	1	51.7	6.26	3.77	0.273	10.5	4.38	0.527
8.31	2	27.7	5.12	3.62	0.594	14.2	5.48	0.659
8.31	3	18.5	4.42	3.24	1.04	19.2	5.90	0.710
8.31	4	13.8	4.00	2.93	1.55	24.5	6.05	0.728
8.31	5	11.0	3.70	2.70	2.11	29.8	6.16	0.741
8.31	6	9.15	3.48	2.50	2.72	35.2	6.21	0.747
24.9	0.5	176	7.38	4.09	0.159	12.4	7.59	0.305
24.9	1	149	8.44	4.78	0.221	13.0	11.5	0.460
24.9	2	82.4	7.45	5.06	0.410	15.9	15.2	0.609
24.9	3	55.5	6.43	4.71	0.704	20.3	16.7	0.669
24.9	4	41.7	5.77	4.35	1.05	25.2	17.4	0.699
24.9	5	34.4	5.31	4.02	1.45	30.3	17.8	0.713
24.9	6	27.8	5.00	3.79	1.85	35.4	18.0	0.723
24.9	7	23.8	4.73	3.58	2.29	40.6	18.1	0.726
24.9	8	20.8	4.54	3.43	2.74	45.9	18.2	0.729
83.1	2	274	11.0	6.83	0.297	19.2	46.1	0.555
83.1	3	185	9.68	6.79	0.466	22.8	52.6	0.633
83.1	4	140	8.67	6.43	0.690	27.2	56.2	0.676
83.1	5	112	8.00	6.11	0.940	32.0	57.9	0.697
83.1	6	93.1	7.45	5.78	1.22	36.9	58.6	0.705
83.1	7	79.8	7.08	5.48	1.50	41.9	59.3	0.713
83.1	8	69.8	6.75	5.23	1.81	46.9	59.7	0.718
83.1	9	62.0	6.48	5.05	2.13	51.9	59.8	0.719
83.1	10	55.8	6.25	4.86	2.45	57.1	59.8	0.720
83.1	11	50.7	6.08	4.72	2.78	62.1	59.8	0.720

Table 1: Numerical results for various boundary conditions. First, second and third columns refer to the total luminosity, boundary temperature and boundary optical thickness. The 4-th through 6-th columns show the numerical results for the quantities at the photosphere, while 7-th through 9-th columns show the numerical results for those at infinity.